THE JOURNAL OF PHYSICAL CHEMISTRY B

ARTICLE

pubs.acs.org/JPCB

How Insoluble Particles Affect the Solutions' Conductivity: A Theory and the Test in NaCl and Chitosan Solutions

Ziqin Rong and Qingling Feng*

Laboratory of Advanced Material, Department of Material Science and Engineering, Tsinghua University, Beijing 100084, P.R. China

ABSTRACT: In this study, we formalize a theory about how insoluble particles in the solution affect the solution electrical conductivity. We propose four corollaries of this theory: (1) the conductivity change is the same as long as the concentration of particles exceeds a certain value; (2) the solution conductivity is irrelevant to the particle size; (3) the increasing temperature weakens the particles' effect on solution conductivity; (4) the heavier the ions in solutions are, the larger the conductivity change caused by particles is. We then prove these four corollaries to be right by experiments in two solution systems, NaCl + $CaCO_3$ and chitosan + nHAC (nanohydroxyapatite/collagen composite).

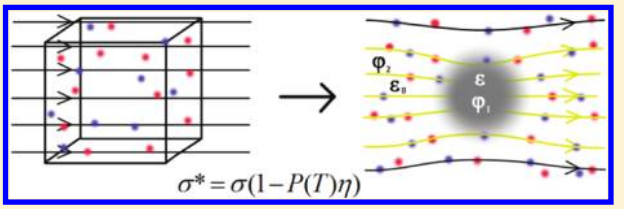

1. INTRODUCTION

The study of conductivity in inhomogeneous media has a long history.[1] Beginning in the 19th century with the development of molecular field concept, it concerns with a set of effective problems in two-phase systems, like thermal conductivity, dielectric constant and electrical conductivity. (Because they all share the same kind of equations: $q = -k\nabla T$, $D = -\varepsilon\nabla\varphi$, $j = -\sigma\nabla\varphi$.) And the increased interest to this problem today is partly triggered by porous thermal barrier coatings[2−7] and substrates for electronic circuit packages.[8,9]

Some of the famous results in this problem include Poisson's theory of induced magnetism, the Clausius−Mossotti theory for the dielectric constant, the Lorenz−Lorentz theory for the index of reflection, etc. The last theory renders the following formula when applied to the case of electric conductivity

$$\frac{k_r - 1}{k_r + 2} = \phi\frac{(k_1/k_0) - 1}{(k_1/k_0) + 2} \tag{1}$$

where ϕ is the volume percentage of the second phase, k_r is the proportion between effective conductivity and medium conductivity, $k_r = k_{eff}/k_0$, k_1 is the particle conductivity.

Equation 1 reduces to the popular Maxwell−Eucken equation.[10−14] When the conductivity of the second phase k_1 is negligible[14]

$$k_r = \frac{1 - \phi}{1 + \phi/2} \tag{2}$$

Furthermore, various editions and extensions have been conducted by scientists on the Maxwell−Eucken relationship. Some of them include more subtle elements into consideration, such as the suspension shape, concentration, AC electrical field, zeta potential, particle surface conditions, etc.[15−29]

Recently, the Coble−Kingery approach[30−32] has been used to derive another predictive relation:

$$k_r = 1 - \frac{3}{2}\phi + \frac{1}{2}\phi^2 \tag{3}$$

However, none of above relationships can account for the saturation phenomena we encountered in our experiments. In chitosan/nHAC system, the solution conductivity change shows no correlation with the nHAC density, while eqs 1−3 all tell us that effective conductivity decreases as we add more insoluble particles into the system. In this paper, by electro-dynamical analysis, we build up a simple theory and provide a new viewpoint to the effective problem. Moreover, we manage to prove this theory in two liquid systems by experiments, NaCl solution + $CaCO_3$ and chitosan solution + nHAC. In experiments, we compare the electrical conductivities before and after the addition of insoluble particles. By seeing how particles change the solution conductivity, it proves that this change agrees with the predictions according to the theory. This paper is meaningful for some composite materials, like biomaterials and ion exchange resins fluidized by NaCl solution

2. THEORETICAL BACKGROUND

In this part, we focus on the basic ideas and predictions of this theory. The mathematics are in Appendix.

2.1. Geometrical Model. In this model, there are several important assumptions. First, we assume that the insoluble particles are small spheres homogeneously distributed in the solution. And there is no chemical reaction in the solution/particle system. Every particle influences its surrounding solution, the shape of which makes up a cube. And all the cubes are

Received: March 15, 2011
Revised: August 6, 2011
Published: September 22, 2011

the same in shape and volume. The particle is at the center of the cube, immersed in positive and negative ions (Figure 1). Because every cube is the same, a single one is enough to picture the whole system.

Then, we assume there is a uniform external electric field $\vec{E}_0$, vertical to a pair of parallel surfaces. The particle will change this field as shown in Figure.2.

Part of the electric field lines end on the surface of the particle. It is these lines that are responsible for the change of solution conductivity, and we are able to calculate them by the Poisson equations $\nabla^2\varphi = -\rho/\varepsilon$.

2.2. Physical Model. Our key equation connecting conductivity with electric field is the microscopic Ohm's law

$$\vec{j} = \sigma\vec{E} \tag{4}$$

This equation exhibits the relationship among current density $\vec{j}$, conductivity σ, and electric field intensity $\vec{E}$. After particles are added in the solution, the macroscopic external voltage U_0 does not change, corresponding to an unchanged external field intensity $\vec{E}_0$. But the microscopic intensity $\vec{E}$ is altered by particles, corresponding to a changed current density $\vec{j}^*$. And by eq 4, $\vec{E}_0$ unchanged, but $\vec{j}$ turns into $\vec{j}^*$, so σ will becomes σ^*. This is the main idea how we calculate the new conductivity.

For the convenience of calculating, we make some assumptions to simplify the situation, the main three ones are as follows:

(1) Particles are homogeneously distributed in solution, and there is no interaction among them, such as collisions, etc.

(2) The size of the cube is macroscopically small and microscopically large, so we may assume the external electric field to be uniform and the ionic charge density in the cube to be zero. Moreover, the particle size is much smaller than that of the cube.

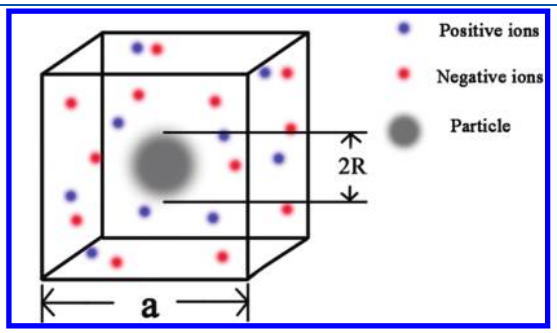

Figure 1. Particle and solution cubic.

(3) We carry out calculations while neglecting the thermal motions of ions. So to speak, all ions move along the field lines, and those ions moving along the surface-ending lines collide onto the particle, we assume the electric current represented by these ions turns into surface current, which move upon the particle surface and leaves it at the other end.

However, there are two limiting situations of which we must be aware: (1) The more particles are in the solution, the more field lines end upon particle surfaces. So when the particle concentration reaches a critical value, all the field lines end on the particle surfaces, meaning that all the electric current becomes surface current. And if we add more particles, all the field lines still end on the particle. So it makes no difference when the particle concentration passes that critical point, and the conductivity change is the same. We call this situation the saturation phenomenon. (2) In the discussion above, we talk about the situation that there is no thermal motion. However, thermal motion of the ions does exist, and the ions may escape from the field lines which they should move along. So a part of ions may escape from their original field lines which end upon the particle and jump to other lines which do not end upon the particle. Therefore, the current represented by these ions does not become surface current. So even in the saturation condition, the conductivity is not zero.

Under these assumptions and considerations, we are able to get the final result about the conductivity after carrying out the calculations in Appendix.

$$\sigma^* = \sigma(1 - P(T)\eta) \tag{5}$$

where σ^* is the solution conductivity after adding insoluble particles, and σ is the one before adding. $P(T)$ is the coefficient of correction accounting for thermal motion effect, $P(T) < 1$. η is a function defined as

$$\eta = 1 \text{ if } 12\pi R^2(cN_A)^{2/3} \geq 1 \tag{6.1}$$

$$\eta = 12\pi R^2(cN_A)^{2/3} \text{ if } 12\pi R^2(cN_A)^{2/3} < 1 \tag{6.2}$$

where R is the average radius of the particles, c is the particle number density, and N_A is the Avogadro's constant. The definition of η accounts for the saturation phenomenon. $12\pi R^2(cN_A)^{2/3}$ stands for proportion of the field lines that end on the particle surface. When $12\pi R^2(cN_A)^{2/3} = 1$, it is just the situation that all field lines end upon the particle.

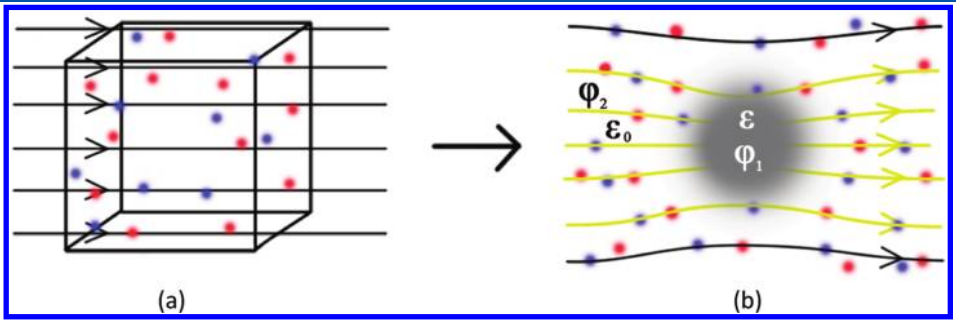

Figure 2. Electronic field changes after adding an insoluble particle, represented by field lines: (a) before addition and (b) after addition. The yellow lines in b represent the surface-ending field lines, which are responsible for the conductivity decrease.

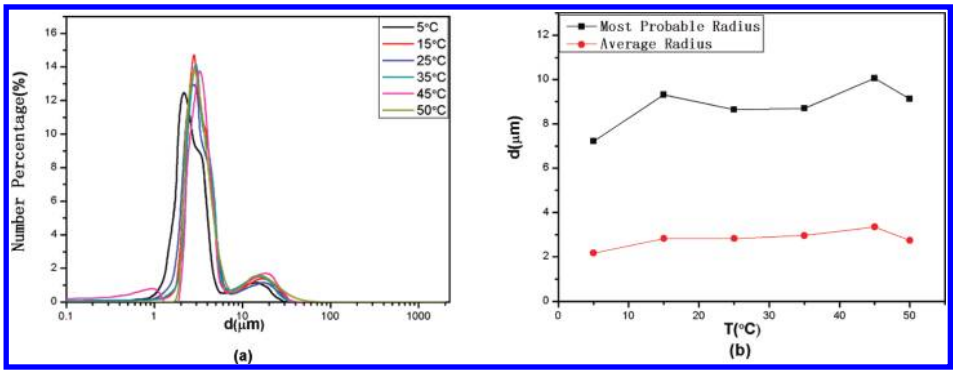

Figure 3. (a) Size distributions at different moments; (b) average and most probable sizes, calculated from information of panel a. Average size corresponding to the volume average, $\bar{r} = (\sum_i r_i^3 x_i)^{1/3}$, i stands for all the data points and x_i is the number percentage of particle with radius r_i. Most probable radius is the radius corresponding to the curve peak in panel a.

2.3. Corollaries of the model. The model above proposes some predictions about the way how insoluble particles change the solution conductivity. Here are the main four corollaries.

(1) The conductivity change is the same as long as the concentration of particles exceeds a certain value. This statement is easily verified because once the particle concentration c surpasses such a critical value, we can see from 6.1 and 6.2 that η becomes 1 and it does not change anymore, resulting in the same change in conductivity according to eq 5. That is the saturation phenomenon.

(2) The solution conductivity is irrelevant to the particle size. Assuming a particle averagely consists of n molecules with r_0 as the radius of each molecule, then $R = n^{1/3} r_0$, $c = c_0/n$, where c_0 is the molecule concentration. Therefore, $R^2 c^{2/3} = r_0 c_0^{2/3}$ is a constant too, implying η does not depend on R and neither does σ^*. So we conclude that the conductivity change does not rely on the particle size.

(3) The increasing temperature weakens the particles' effect on solution conductivity. Because of the thermal motions, ions escape from the electric field lines which they should move along, causing part of the current which should have become surface current escape from the particle surface. Therefore, the higher the temperature is, the more intense thermal motion is, and the more electric current escapes, the smaller $P(T)$. So temperature rise decreases the quantity of $P(T)$.

(4) The heavier the ions in solutions are, the more the change of the solution conductivity is. Because the heavier the ions are, the less intense thermal motion is, therefore $P(T)$becomes larger at the same temperature.

3. MATERIALS AND METHODS

3.1. Materials. We conduct our experiments in two solution systems. The first is a NaCl solution with $CaCO_3$ as the insoluble particles. This is a common inorganic salt solution used in theoretical study. And the second is a chitosan solution, with nHAC (nanohydroxyapatite/collagen composite) as the insoluble particles. It is a biomaterial applied in bone defect repair. The chemicals in analytical pure grade are from Chemical Agents Co., Ltd. (Beijing, China). The water used in the experiments is deionized.

3.1.1. NaCl Solution + $CaCO_3$. This system was created by mixing Na_2CO_3 (0.1 M) and $CaCl_2$ (0.1 M) solutions together.

3.1.2. Chitosan Solution +nHAC. Chitosan is a copolymer combining acetylgluscosamine with glucosamine,[33] a linear cationic polyelectrolyte ($A - H \rightleftharpoons A^- + H^+$) derived by alkaline deacetylation of chitin in crustacean shells.[34] And it is generally acknowledged that chitosan is derived when the fraction of deacetylated monomers is greater than 70%.[35]

3.1.2.1. Chitosan Solution Preparation. A 0.1 M HCl solution was prepared before chitosan powder (Medical grade, M_w 250 000, degree of deacetylation 96.0%, Shandong AK Biotech Ltd., China) was added. The concentration of the chitosan monomers was 0.1 M. Then the solution was stirred by the magnetic stirring apparatus at the medium speed for 24 h to make the chitosan dissolve into the acid solution. Afterward, the solution was kept in the refrigerator at 4 °C. Because of degradation, the usable period of this solution after preparation was within one week.

3.1.2.2. Synthesis of nHAC Powder. The synthesis of nHAC powder has been reported previously.[36] Collagen (Medical grade, type I, YierKang Company, China) was diluted at a concentration of 0.6 mg/mL by 10 mM hydrochloric acid at 4 °C. $CaCl_2$ solution (1.4 mL 0.1 M) was added into 10 mL of collagen solution and maintained for 10 min after mixing. A NaH_2PO_4 solution (0.84 mL 0.1M) was added, and the pH was adjusted to 7.0 by a 0.1 M NaOH solution. When the pH exceeded about 6.0, the solution became supersaturated and calcium phosphate started to precipitate with collagen. The solution was maintained at pH 7.0 for 1 h, after which the composite was harvested by centrifugation at 5000 rpm and suspended in deionized water to remove the salts. The centrifugation and suspension cycle was repeated three times. After the last suspension the sample was freeze-dried. The precipitate was ground into fine powder.

3.2. Methods. We put the solutions in a thermal sink, which is connected to a thermostatic water bath (THGD-0506, High-accuracy Thermostatic Bath, Ningbo, China). Then as we increased the temperature of the bath at a rate about 2 °C/min, the temperature and conductivity were measured at the same time with a pH-conductivity measuring apparatus (DDSJ-308, Shanghai, China). Under the thermal sink was a magnetic stirring apparatus, controlling the mixing speed when we put Na_2CO_3 and $CaCl_2$ solutions together. The particle size was measured by a laser particle analyzer (MasterSizer 2000, Hydro 2000MU).

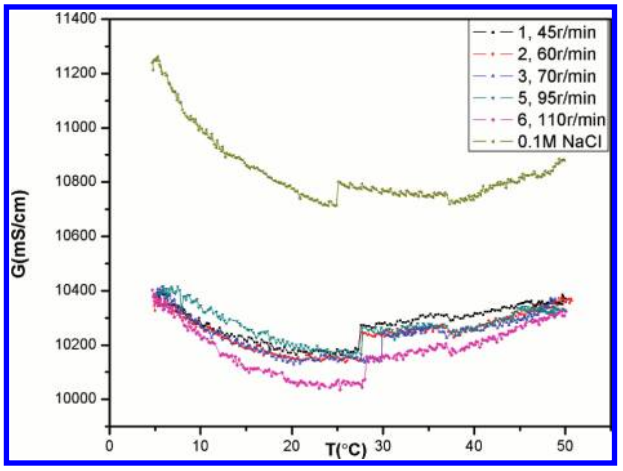

Figure 4. Conductivity of NaCl solution with $CaCO_3$ of different sizes, data taken every 20s. The system was derived from mixing 50 mL of $NaCO_3$ (0.1 M) and 50 mL of $CaCl_2$ (0.1 M) at different speed. 1−6 stands for the speed grade of stirring apparatus at which the two solutions were mixed, and 45*r*/min was the approximate solution rotation rate for grade 1, etc., and 0.1 M NaCl was the pure NaCl solution without $CaCO_3$ for comparison. Temperature increase rate is 2 °C/min.

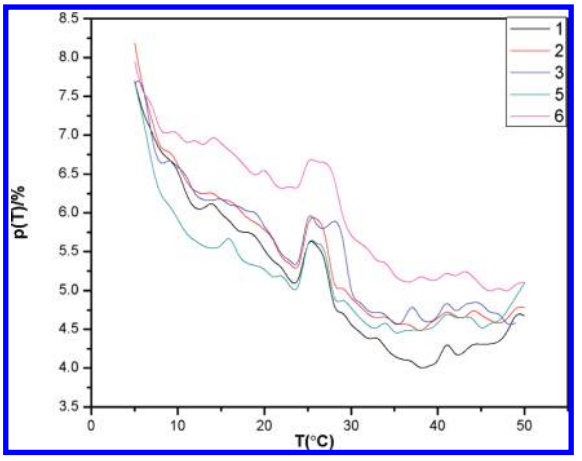

Figure 5. $P(T)$ of NaCl + $CaCO_3$ system. $P(T)$ was calculated from data in Figure.4 by eq 7.

4. RESULTS

4.1. NaCl + $CaCO_3$ System. In this experiment, we mainly want to test how particle size affects the solution conductivity. However, first we should make sure the particle size does not change substantially during the measuring procedure. The experimental condition here is same as the following measurement in Figure 4. 250 mL of Na_2CO_3 (0.1 M) and 250 mL of $CaCl_2$ (0.1 M) solutions were mixed. The system was then cooled to 5 °C, and afterward temperature increases at a rate of 2 °C/min to 50 °C, the particle size were measured at 5, 15, 25, 35, 45, and 50 °C respectively.

The experimental results by laser particle analyzer are positive. In the whole experimental process, the particle size did not change substantially (Figure 3).

A basic fact is that the $CaCO_3$ particle size depends on the speed we mix $NaCO_3$ and $CaCl_2$ solutions. The faster they mix up, the faster the chemical reaction goes, and the smaller the size

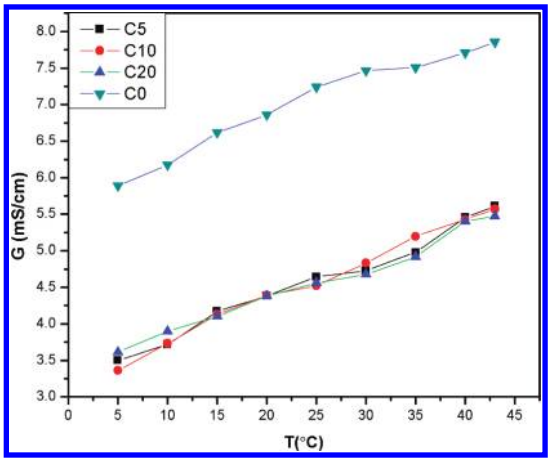

Figure 6. Conductivity change in chitosan-nHAC system. C0, C5, C10, and C20 are 0, 5, 10, and 20 mg/mL nHAC respectively, each sample is 20 mL.

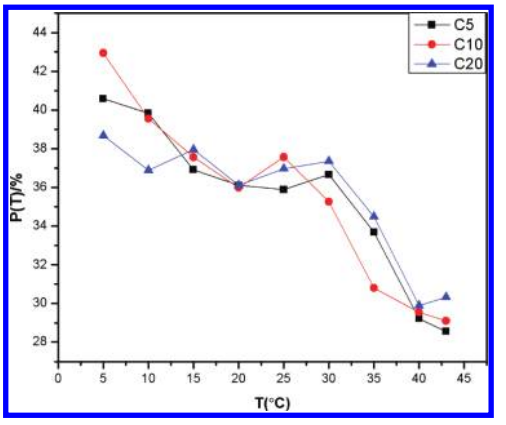

Figure 7. $P(T)$ of chitosan + nHAC system. $P(T)$ was calculated from data in Figure.6 by eq 7.

of $CaCO_3$ is. Groups with different $CaCO_3$ sizes exhibit similar conductivities from 5 to 50 °C (Figure 4). And this is what corollary 2 predicts, that the conductivity change does not rely on the particle size.

The properties of $CaCO_3$ particles satisfy 6.1 and therefore we take $\eta = 1$ and calculate $P(T)$ by

$$P(T) = \frac{\sigma_0 - \sigma^*}{\sigma_0} \tag{7}$$

where σ^* and σ_0 are the conductivities of NaCl solution with and without $CaCO_3$ respectively.

Coordinating with corollary 3, the general trend is that $P(T)$ becomes smaller when temperature rises (Figure 5). And $P(T)$ is not very large for NaCl solution, about 4−8%, indicating a strong thermal-motion correction effect for low-weight ions like Na^+ and Cl^-.

4.2. Chitosan−nHAC System. In this experiment, we mainly want to test corollary 1, the saturation phenomenon, in an organic salt solution system.

The nHAC addition clearly reduces the conductivity, and this decrease is just the effect caused by currents which collide onto nHAC as the theory states. However, concentration of nHAC is irrelevant to the conductivity change (Figure.6). This is

the saturation phenomenon: when the particle concentration passes a certain value, the conductivity change stays the same. To verify that corollary 1 is correct in this system, we prove that nHAC concentration in C5 has already exceeds that value, satisfying 6.1, $\eta = 1$. 70 wt % of nHAC consists of $Ca_{10}(PO_4)_6(OH)_2$. In C5, the concentration of $Ca_{10}(PO_4)_6(OH)_2$ molecules in C5 is $c_0 = 4.98 \times 10^{-3}$ mol/L. Even not taking collagen proteins into account, the radius of every $Ca_{10}(PO_4)_6(OH)_2$ molecule is at least $r_0 = 2 \times 10^{-8}$ m(estimation made from considering the ion radius), then $12\pi r_0^2(c_0N_A)^{2/3} = 3.316 > 1$. And the collagen proteins would only increase r_0 and make $12\pi r_0^2(c_0N_A)^{2/3}$ larger. So in C5, $\eta = 1$. If we put more nHAC, like C10, C20, the conductivity change should be the same due to our corollary 1, which is just the saturation phenomenon, consistent with our experimental results.

Same as in NaCl + $CaCO_3$, we calculate $P(T)$ in this system, and corollary 3 is proved to be right in this organic salt solution too (Figure 7).

The $P(T)$ of this system, about 30−45%, is much larger comparing to that of NaCl + $CaCO_3$, which is about 4−8%. And this is exactly what corollary 4 predicts, because the carriers in this system are chitosan, which have a much larger weight than Na^+ and Cl^-.

5. CONCLUSION

In this study, we formalize a theory, propose corollaries, and prove this theory to be right in two solution systems, an inorganic salt solution (NaCl + $CaCO_3$) and an organic salt solution (chitosan + nHAC). It may be meaningful to do more studies to give a theoretic prediction for the thermal-motion correction coefficient $P(T)$. Moreover, both $P(T)$ of these two systems show a peak between 20 and 30 °C. This phenomenon needs further study for explanation.

APPENDIX

In Figure.1, as all the cubes are the same, the size of the cube, a, is determined from the particle number density

$$cN_Aa^3 = 1 \tag{8}$$

Now we calculate the electric field after adding particles in Figure.2. Assuming the electric potential inside the particle is φ_1, outside the particle is φ_2; and ε the dielectric constant of the insoluble particle, ε_0 the dielectric constant of water. The radius of the particle is R, and we use the spherical coordinates (r,θ,ϕ) with the particle's center as the origin and z axis along E_0. Then the Poisson equations and boundary conditions are

$$\nabla^2\varphi_1 = 0 \quad \nabla^2\varphi_2 = 0 \tag{9.1}$$

$$\begin{aligned} {}''\varphi_1|_{r=R} &= \varphi_2|_{r=R}\varepsilon_0 \frac{\partial\varphi_2}{\partial r}\bigg|_{r=R} - \varepsilon\frac{\partial\varphi_1}{\partial r}\bigg|_{r=R} = s(\theta,\varphi)\varphi_2|_{r\to\infty} \\ &= -E_0r\cos\theta \lim_{r\to 0}\varphi_1 \neq \infty \end{aligned} \tag{9.2}$$

where $s(\theta,\varphi)$ is the surface charge density on the particle surface, and it should be a function of location. Once the external field is applied in the solution, the current begins to flow and the charge starts to build up upon the surface.

Because of the geometrical symmetry of the sphere and electrical field, $s(\theta,\varphi)$ should be a function of θ only and obey the following two restrictions:

$$s(\theta) = -s(\pi-\theta) \quad \int_0^{2\pi} s(\theta)\,d\theta = 0 \tag{10}$$

The second restriction accounts for the total charge neutrality request. So if we expand $s(\theta)$ in Fourier series, we get

$$s(\theta) = s_1\cos\theta + s_2\cos 2\theta + s_3\cos 3\theta + \dots \tag{11}$$

The first term $s_1\cos\theta$ is the charge built up from the original uniform electrical field and it should make up the main part of $s(\theta)$. The higher order terms such as $s_2\cos 2\theta$, $s_3\cos 3\theta$, etc., stands for the charge built up from the electrical field after considering the corrections caused by surface charge $s_1\cos\theta$.

Taking $s(\theta) = s_1\cos\theta$ as the first-order approximation, the solutions to these equations are

$$\begin{cases} \varphi_1 = -\dfrac{3\varepsilon_0E_0 + s_1}{\varepsilon + 2\varepsilon_0} r\cos\theta \\ \varphi_2 = \left[\dfrac{(\varepsilon-\varepsilon_0)E_0 - s_1}{\varepsilon + 2\varepsilon_0}\dfrac{R^3}{r^2} - E_0r\right]\cos\theta \end{cases} \tag{12}$$

Then the electric field intensity on the particle surface is

$$E|_{r=R} = -\nabla\varphi_2|_{r=R} = \frac{3\varepsilon E_0 - s_1}{\varepsilon + 2\varepsilon_0}\cos\theta \tag{13}$$

By applying 1, the electric current colliding upon the particle surface is

$$I' = 2\times\int_0^{2\pi} d\phi\int_{-\pi/2}^{\pi/2} R^2|\sin\theta|d\theta\sigma E|_{r=R} = 4\pi R^2\times\sigma\frac{3\varepsilon E_0 - s_1}{\varepsilon + 2\varepsilon_0} \tag{14}$$

Current I' is the current that turns into surface current according to assumption 3, and the coefficient 2 stands for the double count of both positive and negative ions. The electrical resistivity of this kind current can be divided into two parts: $R_{I'} = R_{\text{solution}'} + R_{\text{surface}'}$, in which $R_{\text{solution}'} \ll R_{surfaXce'}$, because ions and fluid move much harder on surface than in solution. This is because surface viscous force exists and the ions are much denser around surface, so the ions' average free path is much shorter than that in solution. In approximation, we can take $R_{I'} \approx R_{\text{surface}'}$.

For the current $I-I'$, which does not collide onto particle surface (I is the total current, $I = \sigma E_0a^2$), the resistivity is purely $R_{I-I'} = R_{\text{solution}}$ because they only move in solution. And thus the total effective resistivity is

$$\frac{1}{R^*} = \frac{1}{R_{I'}} + \frac{1}{R_{I-I'}} \approx \frac{1}{R_{I-I'}} \quad (R_{\text{solution}} \ll R_{\text{surface}'}) \tag{15}$$

By expressing resistivity in conductivity, we have the equation for calculating effective conductivity σ^*

$$\sigma^*a = \sigma\frac{S^*}{a} \tag{15'}$$

where S^* is the cross-sectional area of "solution" current and we can get S^* from the ratio between $I-I'$ and I, because the current is uniform on the cubic surface

$$\frac{S^*}{a^2} = \frac{I-I'}{I} \tag{16}$$

Then, by some simple calculation, we have the final expression for σ^*

$$\sigma^* = \sigma\left[1 - \left(\frac{3\varepsilon}{\varepsilon + 2\varepsilon_0} - \frac{1}{\varepsilon + 2\varepsilon_0}\frac{s_1}{E_0}\right)\frac{4\pi R^2}{a^2}\right]$$

$$\approx \sigma[1 - (3-\delta)4\pi R^2(cN_A)^{2/3}] \approx \sigma[1 - 12\pi R^2(cN_A)^{2/3}] \quad (17)$$

The last two approximations have used the fact that $\varepsilon \gg \varepsilon_0$ in most situations and δ ($\delta = (1)/(\varepsilon + 2\varepsilon_0)(s_1)/(E_0)$) can be very small, because E_0 is an imaginary electrical field and we can always make it very large.

And with the consideration of the limiting case which we discussed in the Theoretical Background, we have the expression in eqs 5, 6.1, and 6.2.

AUTHOR INFORMATION

Corresponding Author

*Phone: +86-10-62782770. Fax: +86-10-62771160. E-mail: biomater@mail.tsinghua.edu.cn.

ACKNOWLEDGMENT

The authors are grateful for the financial support from the 973 Project (2007CB815604), National Natural Science Foundation of China (51072090, 51061130554) and Doctor Subject Foundation of the Ministry of Education of China (20100002110074).

REFERENCES

(1) Landauer, R. *Electrical, Transport and Optical Properties of Inhomogeneous Media*; American Institute of Physics: New York, 1978; pp 2−43.
(2) Klemens, P. G.; Gell, M. *Mater. Sci. Eng.* **1998**, *A245*, 143–149.
(3) Raghavan, S.; Wang, H.; Dinwiddie, R. B.; Porter, W. D.; Mayo, M. J. *Scr. Mater.* **1998**, *39*, 1119.
(4) Sharafat, S.; Kobayashi, A.; Ogden, V.; Ghoniem, N. M. *Vacuum* **2000**, *59*, 185.
(5) Wang, Z.; Kulkarni, A.; Deshpande, S.; Nakamura, T.; Herman, H. *Acta Mater.* **2003**, *51*, 5319.
(6) Kulkarni, A.; Vaidya, A.; Goland, A.; Sampath, S.; Herman, H. *Mater. Sci. Eng.* **2003**, *A359*, 100.
(7) Cernuschi, F.; Ahmaniemi, S.; Vuoristo, P.; Mantyla, T. *J. Eur. Ceram. Soc.* **2004**, *24*, 2657.
(8) Pezzotti, G.; Kamada, I.; Miki, S. *J. Eur. Ceram. Soc.* **2000**, *20*, 1197.
(9) Boey, F. Y. C.; Tok, A. I. Y. *J. Mater. Process. Technol.* **2003**, *140*, 413.
(10) Eucken, A. *Ceram. Abstr.* **1932**, *11*, 576.
(11) Eucken, A. *Ceram. Abstr.* **1933**, *12*, 231.
(12) Maxwell, J. C. *A Treatise on Electricity and Magnetism*; Clarendon Press: London, 1873; pp 194.
(13) Markov, K. Z. *Heterogeneous Media*; Birkhäuser: Basel, 2000; pp 1−162.
(14) Torquato, S. *Random Heterogeneous Materials—Microstructure and Macroscopic Properties*; Springer: New York, 2002; pp 6−12, 403−463.
(15) Grosse, C.; Delgado, A. V. *Curr. Opin. Colloid Interface Sci.* **2010**, *15*, 145–159.
(16) Grosse, C.; Pedrosa, S; Shilov, V. N. *J. Colloid Interface Sci.* **2003**, *265*, 197–201.
(17) Grosse, C. *Interfacial Electrokinetics and Electrophoresis*; Marcel Dekker: New York, 2002. pp 277−326.
(18) Grosse, C; Shilov, V. N. *J. Colloid Interface Sci.* **2007**, *309*, 28.
(19) Fricke, H. A. *Phys. Rev.* **1924**, *24*, 575–587.
(20) Reynolds, J. A.; Hugh, J. M. *Proc. Phys. Soc.* **1957**, *70*, 769–775.
(21) O'Konski, C. T. *J. Phys. Chem.* **1960**, *64*, 605–619.
(22) Bikerman, J. J. *Trans. Faraday Soc.* **1940**, *36*, 154–160.
(23) Schwan, H. P.; Schwarz, G.; Maczuk, J.; Pauly, H. *J. Phys. Chem.* **1962**, *66*, 2626–2635.
(24) Schwarz, G. *J. Phys. Chem.* **1962**, *66*, 2636–2642.
(25) Ballario, C; Bonincontro, A; Cametti, C. *J. Colloid Interface Sci.* **1976**, *54*, 415–423.
(26) Trukhan, E. M. *Sov Phys Solid State* **1963**, *4*, 2560–2570.
(27) Hill, R. J.; Saville, D. A.; Russel, W. B. *J. Colloid Interface Sci.* **2003**, *263*, 478–497.
(28) Lopez-Garcia, J. J.; Grosse, C; Horno, J. *J. Colloid Interface Sci.* **2003**, *265*, 341–350.
(29) Ahualli, S; Jiménez, M. L.; Carrique, F.; Delgado, A. V. *Langmuir* **2009**, *25*, 1986–1997.
(30) Coble, R. L.; Kingery, W. D. *J. Am. Ceram. Soc.* **1956**, *39*, 377.
(31) Pabst, W.; Gregorova, E. *J. Mater. Sci. Lett.* **2003**, *22*, 959.
(32) Pabst, W.; Gregorova, E. *Ceram.−Silik.* **2004**, *48*, 14.
(33) Roberts, G. A. F. *Chitin Chemistry*; Macmillan: London, 1992.
(34) Hoppe-Seyler, F. *Ber. Dtsch. Chem. Ges.* **1984**, *27*, 3329–3331.
(35) Brugnerotto, J.; Desbrieres, J.; Heux, L.; Mazeau, K.; Rinaudo, M. *Macromol. Symp.* **2001**, *168*, 1–20.
(36) Zhang, W; Liao, S S; Cui, F Z *Chem. Mater.* **2003**, *15*, 3221–3226.